ROTOR BEARING SOLUTIONS INTERNATIONAL, LLC

www.rotorsolution.com

Rotor Drop Analyses and Auxiliary Bearing System Optimization for AMB Supported Rotor/Experimental Validation - Part II: Experiment and Optimization

Prepared by:

RBSI Team

Jianming Cao, Paul Allaire, Tim Dimond

University of Potchefstroom, South Africa

Janse van Rensburg

Cerobear GmbH

Christian Klatt

Rotor Bearing Solutions International, LLC

3277 Arbor Trace

Charlottesville, VA 22911

September 16, 2017

Rotor Drop Analyses and Auxiliary Bearing System Optimization for AMB Supported Rotor/Experimental Validation - Part II: Experiment and Optimization

Jianming CAO*, Paul ALLAIRE*, Timothy DIMOND*, JJ. Janse van RENSBURG** and Christian KLATT***

*Rotor Bearing Solutions International, Charlottesville, VA 22911 USA

E-mail: jianming.cao@rotorsolution.com

**School for Mechanical and Nuclear Engineering, North-West University of Potchefstroom, South-Africa

***CEROBEAR GmbH, Germany

Abstract

This paper forms Part II of the rotor drop analysis, focusing on the auxiliary bearing system design and optimization based on the rotor drop analysis methods, as introduced in Part I. Optimization focuses on shaft orbit, maximum ball bearing stress, and how to avoid possible ball bearing damage due to impact loading during rotor drop by optimizing auxiliary design including bearing selection, preload method, radial and axial damping element, and flexible bearing support. The rotor drop modeling process has been validated with test rig result. Using the detailed rotor drop model and time transient method, simulation results are first compared with test data; and a simulation is presented for an 8-stage horizontal centrifugal compressor, are conducted to investigate the effects of auxiliary bearing design and to optimize the auxiliary system. Axial drops, radial drops and combination of radial/axial drops are all evaluated considering angular contact auxiliary bearing size, number of rows, preload, and flexible damped bearing supports in the axial and radial directions. The rotor drop analysis method introduced in this paper may be used as a design toolbox for the auxiliary bearing system.

Keywords : Rotor Drop; AMB; Auxiliary Bearing; Rotordynamics; Nonlinear Transient Analysis

1. Introduction

Although highly reliable when designed correctly, AMBs do occasionally suffer overloads, equipment power losses, etc. Auxiliary bearings or backup bearings are required by API for active magnetic bearings (AMBs) supported rotor (API 617 8ed, 2014). The auxiliary bearings not only protect the rotor and AMB or other equipment failure, but also provide rotor support under non-operating conditions such as transportation, levitation or test. If AMB system suddenly loses electrical power during operation, the rotor drops and serious internal damage may happen. So a very detailed analysis to evaluate and design an auxiliary bearing system is needed. The clearance between the auxiliary bearing and rotor is typically set to half or less than half the minimum clearance between the rotor and the machine internals (critical clearance) at the AMB, blade or seal locations. Auxiliary bearings are consumable protective devices and can be replaced after several drops.

Time transient methods to simulate the rotor-bearing system have been approached by some researchers focusing on flexible rotor-bearing system (Cao et al, 2015) and roller bearings (Wilkes et al. 2013, Sun 2005, Anders et al. 2013). The testing of auxiliary bearing for AMB has been described (Hawkins et al. 2006, Ransom et al., 2009, Rensburg 2014). Patterns of chaotic jumping, oscillation at the bottom of the auxiliary bearing, excitation of backward whirl, and excitation of forward whirl due to rotor unbalance, rotor weight, and contact friction (Schweitzer, 2009) can occur. The excitation of forward whirl is especially bad; this is a rotordynamic instability driver if it happens. Backwards whirl suppression is also desirable. This orbiting motion is due to contact and friction between shaft/bearing inner surface. The best and most desirable shaft displacement pattern is small amplitudes in the bottom

of the auxiliary bearing clearance. The modeling process described in this paper provides a very useful approach to design successful auxiliary bearing systems.

2. Auxiliary Bearing System

Rolling element auxiliary bearings are the most common solution (Waukesha, Cerobear). The advantages of this kind of bearing include: low friction which minimizes heat and wear, carries both radial and thrust loads, and a minimum volume solution compared with the other types. With the right design and materials, the rolling element bearings don't need lubrication. Rolling element bearings, with steel or ceramic balls and without a cage, reduces the possibility of skidding within the bearing . A typical double row, angular contact ceramic ball bearings designed by Cerobear is shown in Fig.. 1.

A typical auxiliary bearing system design is shown in Fig. 2. In both radial and axial directions, the gap between the inner ring and shaft/sleeve has to be small enough to avoid any contact between AMB rotor and stator or between rotating parts and the housing. During the rotor drop, the orbits and forces will be influenced by the displacements of the inner race, deformation of damping elements, movement of outer races, and increased axial bearing play due to wear of the bearing races.

In general, rolling element auxiliary bearings have almost no damping, also the damping between shaft and inner race during contact is very small due to hard surfaces. So additional damping during rotor drop event needs to be introduced. As shown in Figs. 2&3, exterior damping elements (tolerance rings or o-rings) are employed in the radial direction and an axial spring stack in the axial direction are generally used to provided both soft spring stiffness and sliding damping. The axial spring provides preload to the auxiliary bearing system as well. The preload which acts on the auxiliary bearing has different types: hard, one-sided and hard two-sided, as shown in Fig. 3.

Fig. 1. Cerobear auxiliary ball bearing

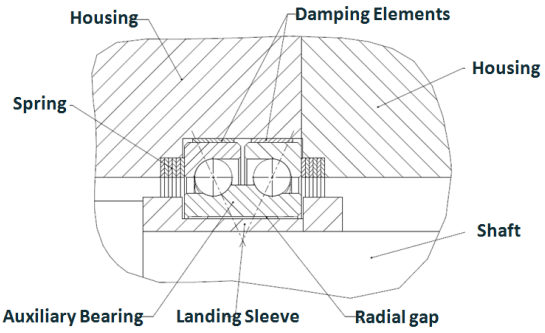

Fig. 2. Typical AUX system

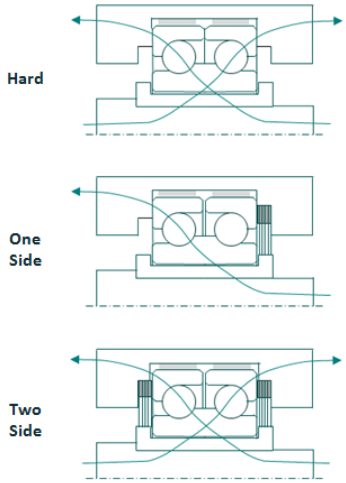

Fig. 3. Preload types for AUX

3. Experimental rotor drop test rig and rotor drop analysis

The rotor drop analysis method and analysis results are firstly compared with an AMB test rig rotor drop experimental data by Rensburg, 2014. This test rig employs two deep groove ceramic ball bearings with cages, which are installed outside of two AMBs as auxiliary bearings as shown in Fig. 4. The rotor information is given in Table 1.

The same rotor was dropped up to 100 times in the same set of auxiliary bearings, with almost same initial condition per drop. The shaft lateral displacement and the shaft rotational speed were measured for each drop. One of the simulation results and test results are shown in Fig. 5. In the left figure, the green line indicates a simulation results, and the blue and red lines indicate the test data. The experimental orbit patterns are similar to the rotor drop model plots for these test results. In Fig. 5 on the right figure, the rate of rotor deceleration is similar between the measured and modeling results for drops 1-8. When the rotor drops more and more times, the shaft speed decreases

faster and faster due to surface friction between shaft and inner race increases.

Table 1. General information of test rig

Rotor weight, kg	7.8
Shaft length, mm	500
Operating speed, rpm	3,000
Shaft diameter at AMB, mm	30
Unbalance, gm-mm	136, 0° @ left AMB 128, 29.7° @ right AMB
Auxiliary bearing	Deep groove ceramic ball bearing Remove all existing lubrication
Shaft-race friction coefficient	0.2
Ball friction coefficient	0.01

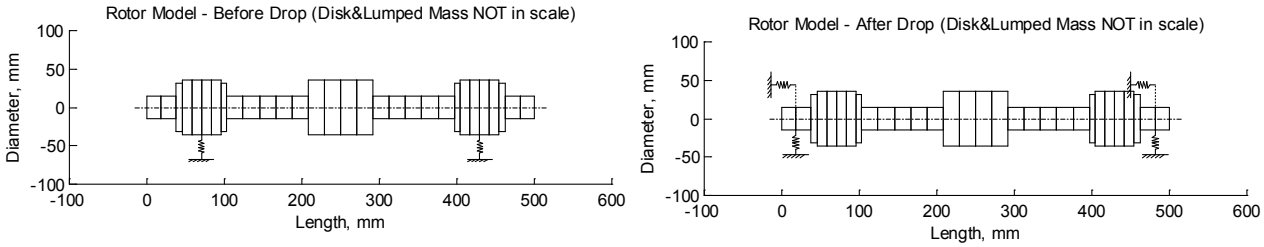

Fig. 4. Test rig rotor model of before and after rotor drop

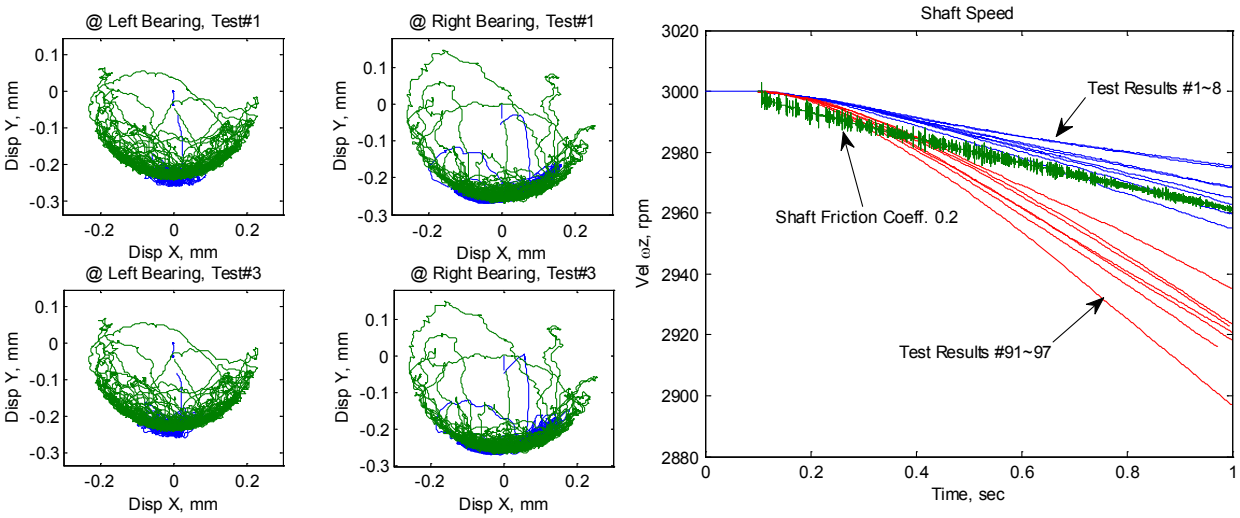

Fig. 5. Shaft orbit compare - simulation (green) and test (blue)

4. Flexible rotor auxiliary bearing system optimization

Another rotor drop example is introduced to illustrate the radial and axial combined rotor drop event and as well as the optimization of the auxiliary system. The same 8-stage centrifugal compressor, as introduced in Part 1, is used for natural gas re-injection at an offshore drilling site. The general properties of the system are listed in Table 3. The rotor has eight compressor impellers attached onto the shaft and it is supported on two radial AMBs and one thrust AMB, as shown in Fig. 6.

Two double row angular contact ceramic ball bearing (one inner race with separated outer race, as seen in Fig. 1) are located next to the radial AMBs as auxiliary bearings. Two-sided axial preload of 3,000N acts onto the outer race

through an axial spring and radial preload of 1000N, added to the outer race through a tolerance ring (See Figs. 2&3). The stiffness and damping of the flexible support is evaluated based upon the geometry and material of axial spring and tolerance ring (Spring-I-Pedia and USA Tolerance Rings). More information about the auxiliary bearing system is listed in Table 3. The unbalance forces act at impellers #4 and #5, counting from the left, with the same phase angle. The rotor is modeled with 30 beam elements and 31 nodes. The curve of total axial load/torque at disks and shaft rotational speed is shown in Fig. 7. During the rotor drop event, radial and thrust AMBs lose power, then the AUXs take both radial and axial loads. There is no torque to drive the rotor from the drive end, however the axial loads and torques at disks still exist and follow the curve in Fig. 7. as the shaft rotational speed is decreasing.

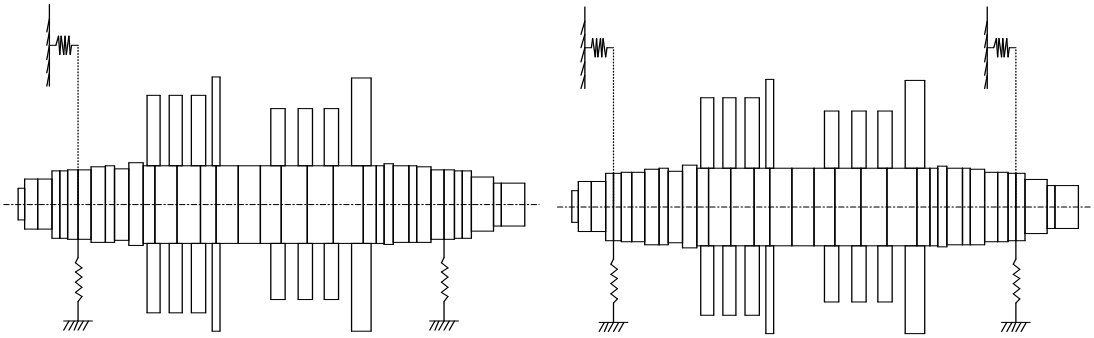

Fig. 6. 8-stage flexible rotor model with AMBs, before and after drop

Table 2. General information of 8-stage compressor

Number of disks	8
Rotor weight, kg	1319.3
Shaft length, mm	2959.1
Operating speed, rpm	8,000
Shaft diameter at AMB, mm	152.4
Unbalance, kg-m	1.05E-3*2 @ disk4&5
Start time, s	0
Drop time, s	0.2
End Tim, s	1.0
Time step, s	8.0E-6

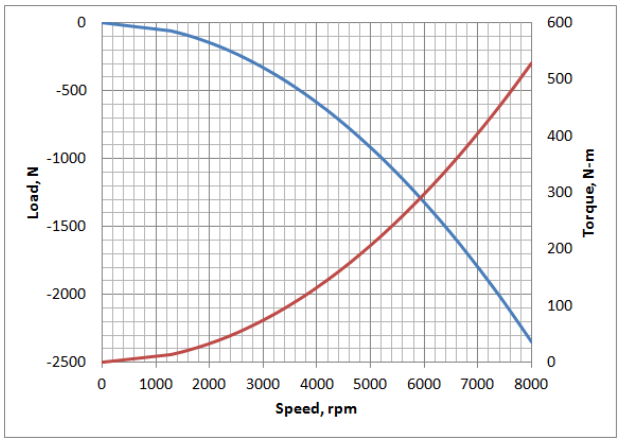

Fig. 7. Axial load and torque vs. speed

Table 3. Specifications of 150mm ball bearing

Double row angular contact ceramic ball bearing	
Bore diameter, mm	150
Outside diameter, mm	210
Width, mm	56
Ball diameter, mm	19.05
Number of balls per row	26
Inner and outer race curvature	0.548 & 0.528
Initial contact angle, deg	25
Axial preload, N	3000, two-side
Radial preload, N	1000
Number of row	2
Friction coefficient, sliding &rolling	0.1 & 0.01
Radial support stiffness, N/m	190E6
Radial support damping, N-s/m	2500
Axial support stiffness, N/m	15E6
Axial support damping, N-s/m	5000
Shaft-race friction, static and kinetic	0.5 & 0.3
Radial gap, mm	0.5
Axial gap, mm	1.0
Maximum contact damping, N-s/m	500

The whole shaft node point orbits of period of 0~0.5sec (drop at 0.1sec) are shown in Fig. 8, the blue lines indicate the nodal position before rotor drop, and the red lines are orbits during rotor drop event. In the axial direction, the analysis results of modeling with and without axial flexible supports is given in Fig. 9. The existence of the flexible

support makes the shaft have a fast decay rate after each impact. The shaft orbits at the two auxiliary bearing are shown in Fig. 10. From the results, there are no large shaft orbits, and the rotor drops onto the bottom area of the AUXs for this case. The maximum radial displacement at the auxiliary bearing is 0.65mm, including air gap of 0.5mm (red circle in figures). The relative orbits of shaft and inner race indicate that the soft bearing support has much more deformation than the auxiliary bearing itself, as shown in Fig. 11.

The maximum bearing stress is found at left row of the left auxiliary bearing (drive end) since the axial load is from discharge end to drive end. The maximum bearing stress of 2,550MPa occurs at the first several touchdowns, as shown in Fig. 12. An acceptable practical upper limit for steel ball bearing stresses is 3,449MPa for short time periods (Harris, 2007). So the calculated ball bearing stress is less than this limit. The ceramic ball bearing has a higher upper limit than the steel ball bearing. To have a more safe margin, the steel ball bearing limit is used here for design purposes.

5. Optimization of Support Properties Through Modeling Process

The optimization of the spring stiffness support is carried out through the modeling process. The tolerance ring design is approached by varying the stiffness of the tolerance ring. The stiffness of tolerance ring can be modified by pinching the material, thickness, height and distance etc. Three more cases of 1) no ring, 2) 0.25x stiffness ring, and 3) 0.5x stiffness ring are calculated and compared with 4) the chosen ring (1.0x stiffness) used in the previous analysis. All cases have same preload and the same axial spring. The orbits at the auxiliary bearing under different ring stiffness values are shown in Fig. 13.

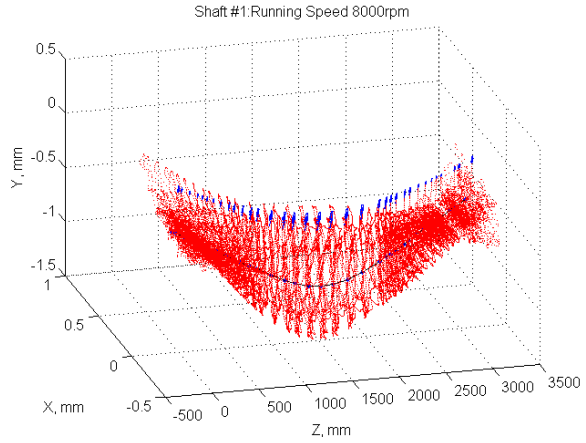

Fig. 8. Orbits of the whole shaft

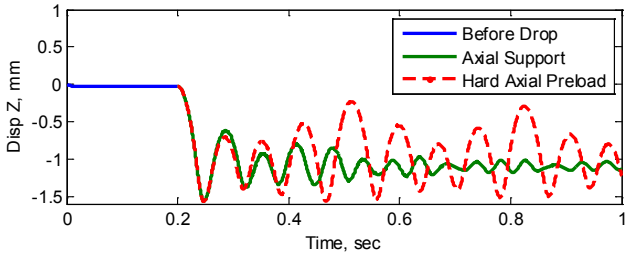

Fig. 9. Axial response at AUX

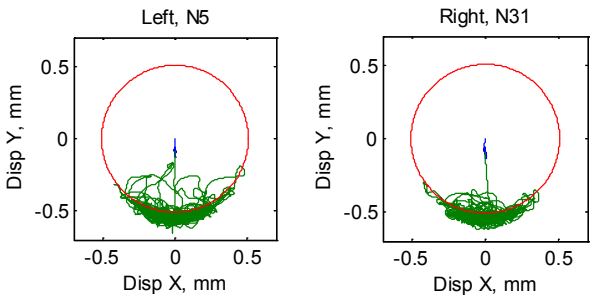

Fig. 10. Shaft orbits at AUXs

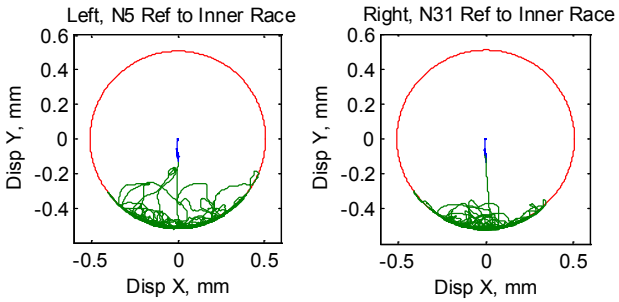

Fig. 11. Shaft orbits at AUXs relative to inner race

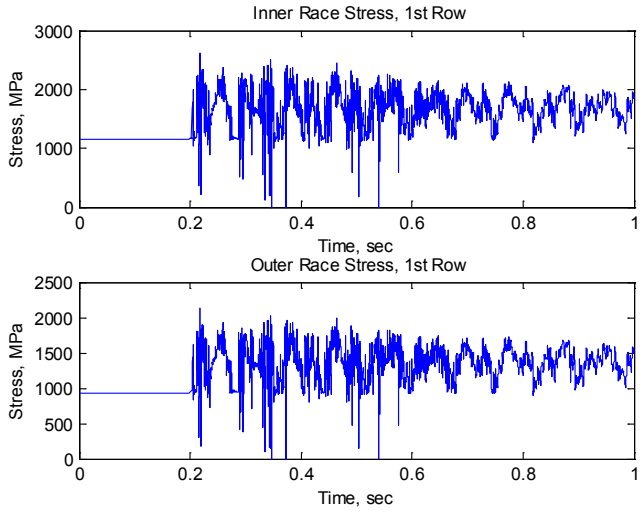

Fig. 12. Maximum bearing stress

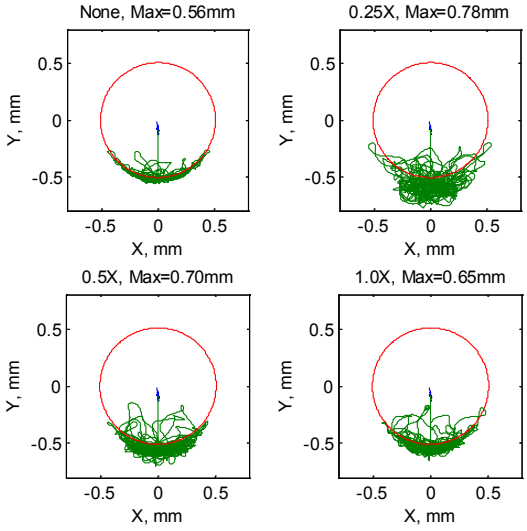

Fig. 13. Shaft orbits under different tolerance rings

The maximum radial displacements are 0.56mm, 0.78mm, 0.70mm and 0.65mm for the four cases, as shown in Fig. 13. The maximum radial displacements are all less than the specified critical rotor/stator clearance of 1.0mm. All cases have small shaft orbits and the shaft orbits are located only in the bottom area of the auxiliary bearing. Considering a typical safety factor of 2.0 (the maximum auxiliary system deformation should less than half of ball bearing air gap), the 0.25X case is not satisfied (0.78mm>0.75mm).

The maximum bearing stresses are 2700MPa, 2300MPa, 2450MPa, and 2600MPa for those four cases. Adding a radial ring increases radial displacement and decreases bearing stress. The worst case is the no ring case. The change of ball bearing stress is very strong in the four cases for this compressor but the lowest value is 0.5X, where 0.25X has been eliminated from the selection above. The main reason that the stresses are not so important in this case is that axial spring has much lower stiffness than radial ring (Table 5), and the stress is depends on the radial and axial motion of inner and outer races. Since tolerance ring with radial preload provides not only radial stiffness and damping, but also axial friction damping due to the outer race axial motion, the tolerance ring is recommended.

6. Conclusion

The paper presents design and optimization of auxiliary bearing system based on rotor drop analysis as well as validation of the model compared to experimental testing was carried out. Detailed information, such as shaft orbits, contact force, and bearing stress, are given through analysis. The analysis results can be use to evaluate contact forces, bearing stresses and affect of flexible support, and to better design auxiliary bearing systems. A comparison of test rig data and simulation results was approached first. The simulated deformation and shaft speed matched the test data reasonably well.

An 8 stage industrial compressor was utilized to radial and axial drop analysis and auxiliary bearing system optimization of an eight stage compressor. The analysis results show that the angular contact preload and flexible support have a very important role in auxiliary system. A properly designed bearing flexible support increases shaft orbit by a small amount, but decreases number of impacts, especially axial touchdown, contact force, and bearing maximum stress.

References

American Petroleum Institute, API Standard 617, 8ed, 2014, "Axial and Centrifugal Compressors and Expander-compressors for Petroleum, Chemical and Gas Industry Services",. Washington, D.C

Cao, J., Dimond, T. W., and Allaire P. E., 2015, "Coupled Lateral and Torsional Nonlinear Transient Rotor-Bearing System Analysis with Applications", ASME J. Dyn. Sys., Meas., Control, 137(9): 091011-091011-9

Wilkes, J., Moore, J., Ransom, D., and Vannini, R., 2013, “An Improved Catcher Bearing Model and an Explanation of

the Forward Whirl/Whip Phenomenon Observed in Active Magnetic Bearing Transient Drop Experiments", ASME J. Eng. Gas Turbines Power, 136(4), 042504

Sun, G, 2005, "Auxiliary Bearing Life Prediction Using Hertzian Contact Bearing Model", ASME J. Vib. Acoust., 128(2), pp203-209

Anders, J, Leslie, P., and Stacke, L., 2013, "Rotor Drop Simulations and Validation With Focus on Internal Contact Mechanisms of Hybrid Ball Bearings", ASME Turbo Expo 2013, GT2013-95816, June 3-7, 2013, San Antonio, TX, USA.

Hawkins, L., Filatov, A., Imani, S., and Prosser, D., 2006, "Test Results and Analytical Predictions for Rotor Drop Testing of an AMB Expander/Generator" ASME J. Eng Gas Turbines Power, vol. 129, pp. 522-529

Ransom, D., Masala, A., Moore, J., Vannini, G., and Camatti, M., 2009, "Numerical and Experimental Simulation of a Vertical High Speed Motorcompressor Rotor Drop onto Catcher Bearings", J. Sys. Design Dynamics, 3(4), pp. 596–606

Rensburg., J, 2014, "Delevitation Modelling of an Active Magnetic Bearing Supported Rotor", PhD Thesis, North-West University, South Africa

Schweitzer, G. and Maslen, E., eds., 2009, "Magnetic Bearings: Theory, Design, and Application to Rotating Machinery", Springer-Verlag, Berlin

Sun, G., 2008, "Auxiliary Bearing Design Guides in Active Magnetic Bearing System", VDM Verlag, Deutschland, Germany

Waukesha Bearings Corp., "Auxiliary Bearing Technology", from http://www.waukbearing.com

Cerobear GmbH, "Auxiliary Rolling Bearing Solutions", from http://www.cerobear.com/index.php?id=248&L=1

Harris, T. A., and Kotzalas, M. N., 2007, "Rolling Breaing Analysis: Essential Concepts of Bearing Technology", 5th Ed., Taylor & Francis Group, New York, NY

Spring-I-Pedia, "Belleville Washers: Formulas", from http://springipedia.com/belleville-washers-formulas.asp

USA Tolerance Rings, "how-tolerance-rings-work", from http://usatolerancerings.com